Lab on a Chip

View Online
Dynamic Article Links

Cite this: DOI: 10.1039/c0lc00392a

www.rsc.org/loc

TECHNICAL NOTE

UV polymerization of hydrodynamically shaped fibers†

Abel L. Thangawng, Peter B. Howell, Jr, Christopher M. Spillmann, Jawad Naciri and Frances S. Ligler*

Received 9th September 2010, Accepted 15th December 2010
DOI: 10.1039/c0lc00392a

Most natural and man-made fibers have circular cross-sections; thus the properties of materials composed of non-circular fibers are largely unexplored. We demonstrate the technology for fabricating fibers with predetermined cross-sectional shape. Passive hydrodynamic focusing and UV polymerization of a shaped acrylate stream produced metre-long fibers for structural and mechanical characterization.

Materials composed of stacked plates, such as abalone shells or even brick walls, are stronger than the same materials in bulk.[1] However, such stacked plate materials are generally composed of hard, inorganic materials cemented together by a more flexible substance and do not occur in long fiber shapes. Very few natural or man-made materials are composed of stacks of plate-like fibers. If such flat, stackable fibers existed, could they be assembled into ultra-strong fiber bundles or fabrics?

Man-made polymer fibers are nearly always round because they are fabricated using two-phase systems; for example, a solubilized polymer precursor or a monomer–initiator solution is introduced into air by electrospinning, extrusion or pulling.[2–8] Hydrodynamic focusing using microfluidic systems has been reported for making solid or hollow, round fibers with micron and sub-micron diameters.[9–15] Lan *et al.* fabricated 300–900 micron tubes with adjustable wall thicknesses using multiple annular flows.[16] The fibers and tubes have been polymerized using both chemical initiators and UV polymerization. Hydrodynamic focusing has also been used to precipitate fibers in microfluidic channels as two reactive streams intersect. These fibers are roughly rectangular, as a result of the shape of the interface between the two streams. Similarly, the barcoded fiber strips produced by Kim *et al.* are rectangular because they are derived from laminar streams aligned in parallel.[17] One other example of non-round fibers was originally reported in 1995[18] and was produced by co-extrusion of polymers with different melting temperatures (www.fitfibers.com). Removal of one polymer produced tri-lobed and deep-grooved fibers advantageous for wicking textiles and for thermal and acoustic insulations.

Hydrodynamic focusing can be performed using grooves in the walls of microfluidic channels to focus one stream with another to create cross-sectional stream shapes more complex than simply circular or rectangular.[19,20] Mott *et al.* developed software that selects the number and shape of grooves that can be placed on opposite sides of a channel to direct two laminar flow streams to achieve a final, *predetermined* distribution of the two fluids with respect to each other.[21] We have used this software to design microfluidic devices producing highly interdigitated streams for mixers or to completely ensheath one stream with another without mixing for microflow cytometry applications.[22] Howell *et al.* demonstrated that five streams could be sequentially introduced between groove sets so that each successively introduced stream completely surrounded the previously introduced streams.[23] The potential to polymerize such concentric tubes and other complex shapes into fibers with well-defined cross-sectional shapes offers intriguing possibilities for materials with a wide variety of applications, including high strength materials, wound healing dressings, controlled release materials, tissue engineering supports, or anti-ballistic fabrics.

In an initial demonstration of production of polymer fibers with pre-designed cross-sectional shapes, we cast acrylate fibers using a hydrodynamic focusing device with grooves in the top and bottom of a microfluidic channel that focused a miscible sheath fluid around the solubilized polymer core solution.[24] Laminar flow minimized mixing of the sheath and core fluids, and hydrodynamic focusing of the sheath fluid controlled the cross-sectional shape of the core. The cross-sectional size was determined by the flow-rate ratio of the core and sheath streams. The fiber hardened as the solvent diffused out of the core into the sheath fluid after the hydrodynamic shaping process and during subsequent flow through the microfluidic channel. However, the range of fiber diameters that could be produced using this casting process was limited. The larger fibers tended to harden first on the outside, leading to collapse of the fibers as the internal regions shrunk during casting. The smallest diameter that could be achieved (~300 nm) was limited by the ability of the pumps to transport the viscous fluids without pulsing. The slow rate of hardening also meant that the fibers tended to become rounder after exiting the microfluidic channel.

Naval Research Laboratory, 4555 Overlook Ave, SW Washington, DC, USA 20375. E-mail: frances.ligler@nrl.navy.mil; Fax: +1 202 404 8897; Tel: +1 202 404 6002

† Electronic supplementary information (ESI) available: Experimental details, COMSOL models of fluid flow in the fabrication device, and raw data from the mechanical analysis. See DOI: 10.1039/c0lc00392a

Report Documentation Page

Form Approved
OMB No. 0704-0188

1. REPORT DATE	2. REPORT TYPE	3. DATES COVERED
2011		**00-00-2011 to 00-00-2011**

4. TITLE AND SUBTITLE	5a. CONTRACT NUMBER
UV polymerization of hydrodynamically shaped fibers	5b. GRANT NUMBER
	5c. PROGRAM ELEMENT NUMBER
6. AUTHOR(S)	5d. PROJECT NUMBER
	5e. TASK NUMBER
	5f. WORK UNIT NUMBER
7. PERFORMING ORGANIZATION NAME(S) AND ADDRESS(ES) **Naval Research Laboratory,4555 Overlook Ave, SW, ,Washington,DC,20375**	8. PERFORMING ORGANIZATION REPORT NUMBER
9. SPONSORING/MONITORING AGENCY NAME(S) AND ADDRESS(ES)	10. SPONSOR/MONITOR'S ACRONYM(S)
	11. SPONSOR/MONITOR'S REPORT NUMBER(S)

12. DISTRIBUTION/AVAILABILITY STATEMENT
Approved for public release; distribution unlimited

13. SUPPLEMENTARY NOTES

14. ABSTRACT

Most natural and man-made fibers have circular cross-sections; thus the properties of materials composed of non-circular fibers are largely unexplored. We demonstrate the technology for fabricating fibers with predetermined cross-sectional shape. Passive hydrodynamic focusing and UV polymerization of a shaped acrylate stream produced metre-long fibers for structural and mechanical characterization.

15. SUBJECT TERMS

16. SECURITY CLASSIFICATION OF:			17. LIMITATION OF ABSTRACT	18. NUMBER OF PAGES	19a. NAME OF RESPONSIBLE PERSON
a. REPORT	b. ABSTRACT	c. THIS PAGE			
unclassified	**unclassified**	**unclassified**	**Public Release**	**4**	

Standard Form 298 (Rev. 8-98)
Prescribed by ANSI Std Z39-18

To overcome these limitations, here we explore UV polymerization as a faster, more uniform method of polymerizing fibers during the hydrodynamic shaping process. The initial challenge was to determine conditions under which the UV polymerization could be accomplished fast enough to lock in the cross-sectional shape of the fiber before it exited the microfluidic channel. The roles of flow velocity, flow-rate ratio, and UV power in creating fibers with rectangular cross-sectional shapes were explored. The microfluidic sheath flow system successfully shaped an acrylate mixture into flat fibers using hydrodynamic focusing and UV polymerization. Initial measurements of the structural and mechanical properties demonstrated shape control and fiber integrity.

Experimental

The design, fabrication and operation of the microfabrication device and COMSOL simulations of the fluid flows within the device are described in the ESI†. The acrylate solution was prepared as follows: 4-hydroxybutyl acrylate (85 wt%), acrylic acid (11 wt%), ethylene glycol dimethacrylate (1 wt%) and photoinitiator (2,2-dimethoxy-2-phenylacetophenone, 3 wt%). All components were in liquid form when combined with the photoinitiator dissolved in dichloromethane at a stock concentration of 1 g mL^{-1}. All chemicals were obtained from Sigma-Aldrich. Prior to mixing the solutions, the hydroquinone inhibitor was removed from the acrylate components using an inhibitor removal column (column SDHR-4 from Scientific Polymer Products, Inc., Ontario, NY). The sheath solution was prepared by mixing glycerol (50 v%), methanol (25 v%), and water (25 v%). The viscosities of the sheath and sample solutions, approximately 10 cP, were measured using a digital viscometer (DV-E, Brookfield Engineering Laboratories Inc., Middleboro, MA). Details of the methods for structural and mechanical characterization are provided in the ESI†.

Results and discussion

Fig. 1 shows scanning electron microscope images of representative fibers obtained at different sheath-to-sample flow-rate ratios. The dimensions of the fibers are tabulated in Table 1. Fibers with dimensions (width × height) from 198 μm × 45 μm to 12.2 μm × 2.6 μm were demonstrated. As evident from these images, the actual cross-sectional shapes of the fibers obtained were in general agreement with those of the COMSOL simulations (Figure 2S, ESI†), both in terms of shape and size for those obtained at slower flow-rates. It should also be noted that the cross-sections of the three larger fibers were very uniform for each set of flow conditions, with coefficients of variation (CVs) of 7–14% in width and height measurements. The two smaller fibers exhibited more variation in cross-sectional measurements (25–38% CVs). Two factors account for the differences in the consistency of the fiber dimensions. First, the 3 larger fibers were fabricated by adjusting the flow rate of the acrylate solution from 3 to 12 μL min^{-1}, while maintaining the sheath flow rate at 300 μL min^{-1}. Since 3 μL min^{-1} was the minimum pump rate, further increases in the flow-rate ratios required increasing the sheath flow rate to 600 μL min^{-1} and 900 μL min^{-1}. Pumping the core against the back pressure from an increasingly strong sheath flow in part accounted for the decrease in the consistency and the greater variation in fiber dimensions. The second factor that may have contributed to the variability was the decreased UV exposure time for the two smaller fibers (Table 1).

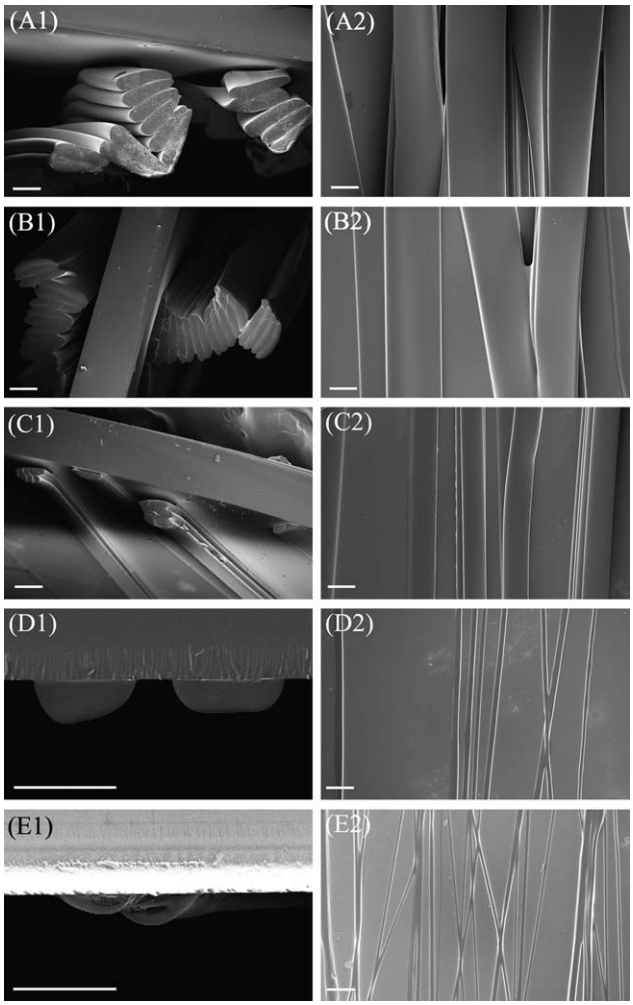

Fig. 1 Scanning electron microscope images of shaped, polymerized acrylate fibers at sheath-to-sample flow-rate ratios of (A) 300 : 12 [25 : 1], (B) 300 : 6 [50 : 1], (C) 300 : 3 [100 : 1], (D) 600 : 3 [200 : 1], and (E) 900 : 3 [300 : 1]. Numbers indicate actual flow rates of the sheath : acrylate in μL min^{-1} and [reduced ratio]. Scale bars: 100 μm (A–C, D2, E2), 20 μm (D1, E1). Fibers were manually wound onto glass coverslips.

The UV exposure time was definitely a factor in choosing the experimental conditions, especially the sheath flow rate. Interestingly, we observed that a minimum exposure time was required to initiate the polymerization process for the acrylate solution. Even when the UV intensity was increased to 8 W cm^{-2} by placing the light guides directly on the channel surface, no polymerization was observed unless the exposure time was approximately 0.5 seconds or more. This is, however, not out of the ordinary as there is a minimum required exposure to initiate polymerization as shown with other polymers.[25] It was desirable to maintain the same exposure time (UV dosage) for all fibers if their material properties were to be compared. For that reason, the first three samples were fabricated with a constant sheath

Table 1 Dimensions of fibers as a function of sheath and sample flow rates

Flow Rates (Sheath : Sample) [μL/min] (reduced ratio)	Fiber Width [μm]	Fiber Height [μm]	UV Exposure time[a] [s]	Simulated Fiber Dimensions[b] Width × Height [μm]
300 : 12 (25 : 1)	198 ± 27	45 ± 6	5.8	188 × 52
300 : 6 (50 : 1)	173 ± 17	30 ± 2	5.9	177 × 48
300 : 3 (100 : 1)	95 ± 10	31 ± 4	5.9	132 × 39
600 : 3 (200 : 1)	21 ± 8	7 ± 2	3.0	84 × 32
900 : 3 (300 : 1)	12 ± 3	2.6 ± 0.7	2.0	70 × 28

[a] Approximate UV exposure time during the polymerization process using a 1000 μm [*W*] × 750 μm [*H*] × 4000 μm [*L*] channel. [b] Fiber sizes were measured from the COMSOL concentration plots at the transition from core to sheath at approximately the 85% diffusion boundary.

flow rate of 300 μL min^{-1}. At 300 μL min^{-1} and a channel geometry of 1000 μm × 750 μm, the linear flow velocity was approximately 6.9 mm s^{-1}, which translated to an exposure time of ~5.8 s (Table 1). Since the pump did not allow the sample flow rate of below 3 μL min^{-1}, the sheath flow rate was increased to obtain smaller fibers. Further increases in the sheath flow rate to reduce the fiber size decreased the exposure time to the point that fibers were not polymerized adequately to maintain their integrity.

The impact of the reduced exposure time on shape retention can also be seen in comparison of the shapes of the smaller fibers in Fig. 1D and E. The fibers in Fig. 1E are rounded to form a semi-cylindrical shape, suggesting that they were not completely polymerized at the time they were wound on the glass slide. Transported into a two-phase environment (*e.g.* gel/air), the fiber interface would adjust to minimize the interfacial tension, causing the fiber to become rounder on the side exposed to the air.

The mechanical properties of the photopolymerized fibers fabricated at a flow rate of 300 μL min^{-1} sheath flow to 12 μL min^{-1} acrylate solution were determined by subjecting multiple fibers to force while monitoring the strain. The initial tensile modulus of the fibers at 30 °C was found to be 6.1 MPa, as shown in Fig. 2A (solid black curve). This value is on par with the estimated tensile modulus of round acrylate-based fibers also created using a microfluidic photopolymerization method.[12] Thus the *in situ* polymerization process described here is sufficient to produce robust fibers with viscoelastic properties.

Subsequent stress/strain cycles were performed to evaluate the viscous loss of the fibers as they are subjected repeatedly to tensile stress. An immediate observation was a notable decrease in the tensile modulus of the fiber bundle to ~2.8 MPa with the successive application of a tensile stress (Fig. 2A, dashed red curve). Such an observation suggests polymer training or annealing of the fibers, a well-established process whereby the polymer backbone is relieved of internal stresses. Analysis of the viscous loss of the fibers with eight successive passive work loops revealed a significant non-linear decrease from 12.2 J kg^{-1} to 8.6 J kg^{-1} (Fig. 2B). The leveling off of the calculated viscous loss with repeated work loops further supports the concept that repeated application of tensile stress continued the annealing of the fibers. Taken together, the mechanical evaluation of these materials indicates we have successfully created stable, flat polymeric fibers *via* UV photopolymerization using a microfluidic approach.

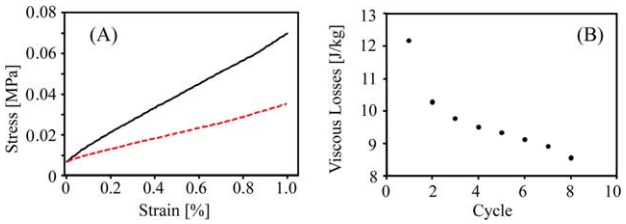

Fig. 2 Mechanical analysis of bundled fibers. (A) Tensile modulus during the first application of force (solid black curve) and final cycle of passive work loop (dashed red curve). (B) Viscous loss of fibers with successive applications of force. See Fig. S3 in the ESI† for the raw data.

Conclusions

Hydrodynamic focusing using passive wall structures was used to shape a prepolymer stream, which was subsequently polymerized using UV exposure. The shape designed using flow simulations was maintained, and the size of the fibers was controlled using the ratio of the flow rates of the sheath and the prepolymer. The fibers exhibited reproducible shapes over metre lengths. The fidelity of the shape was a function of both exposure time and phase matching of the sheath and prepolymer fluids. This microfluidic approach for production of fibers with defined cross-sectional shape can produce fibers for further development of materials with new or improved performance characteristics.

Acknowledgements

This work was funded by NRL/ONR MA 042-06-41 WU 9899 and the Defense Threat Reduction Agency. AT was a National Research Council Postdoctoral Fellow. The views are those of the authors and do not represent the opinion or policy of the US Navy or the Department of Defense.

References

1 F. D. Fleischli, M. Dietiker, C. Borgia and R. Spolenak, *Acta Biomater.*, 2008, **4**, 1694–1706.
2 Y. Srivastava, M. Marquez and T. Thorsen, *J. Appl. Polym. Sci.*, 2007, **106**, 3171–3178.
3 C. R. Carlisle, C. Coulais and M. Guthold, *Acta Biomater.*, 2010, 6, 2997–3003.
4 L. Shor, S. Guceri, R. Chang, J. Gordon, Q. Kang, L. Hartsock, Y. H. An and W. Sun, *Biofabrication*, 2009, **1**, 15003–15010.
5 S. Shin, J. Y. Park, J. Y. Lee, H. Park, Y. D. Park, K. B. Lee, C. M. Whang and S. H. Lee, *Langmuir*, 2007, **23**, 9104–9108.
6 F. X. Gu, L. Zhang, X. F. Yin and L. M. Tong, *Nano Lett.*, 2008, **8**, 2757–2761.

7 S. Ramakrishna, K. Fujihara, W. E. Teo, T. Yong, Z. W. Ma and R. Ramaseshan, *Mater. Today (Oxford, U. K.)*, 2006, **9**, 40–50.
8 A. Tambralli, B. Blakeney, J. Anderson, M. Kushwaha, A. Andukuri, D. Dean and H. W. Jun, *Biofabrication*, 2009, **1**, 025001–025011.
9 E. Shapiro, D. Drikakis, J. Gargiuli and P. Vadgama, *Int. Conf. Nanochannels, Microchannels Minichannels, Proc., 4th*, 2006, 829–836.
10 C. C. Chang, Z. X. Huang and R. J. Yang, *J. Micromech. Microeng.*, 2007, **17**, 1479–1486.
11 C. Ohm, C. Serra and R. Zentel, *Adv. Mater.*, 2009, **21**, 4859–4863.
12 W. Jeong, J. Kim, S. Kim, S. Lee, G. Mensing and D. J. Beebe, *Lab Chip*, 2004, **4**, 576–580.
13 E. Jo, S. W. Lee, K. T. Kim, Y. S. Won, H. S. Kim, E. C. Cho and U. Jeong, *Adv. Mater.*, 2009, **21**, 968–972.
14 M. Marimuthu, S. Kim and J. An, *Soft Matter*, 2010, 6, 2200–2207.
15 E. Kang, S. J. Shin, K. H. Lee and S. H. Lee, *Lab Chip*, 2010, 10, 1856–1861.
16 W. J. Lan, S. W. Li, Y. C. Lu, J. H. Xu and G. S. Luo, *Lab Chip*, 2009, **9**, 3282–3288.
17 S. R. Kim, H. J. Oh, J. Y. Baek, H. H. Kim, W. S. Kim and S. H. Lee, *Lab Chip*, 2005, **5**, 1168–1172.
18 B. M. Philips and W. A. Haile, *Tappi J.*, 1995, **78**, 139–142.
19 P. B. Howell, J. P. Golden, L. R. Hilliard, J. S. Erickson, D. R. Mott and F. S. Ligler, *Lab Chip*, 2008, **8**, 1097–1103.
20 P. B. Howell, D. R. Mott, S. Fertig, C. R. Kaplan, J. P. Golden, E. S. Oran and F. S. Ligler, *Lab Chip*, 2005, **5**, 524–530.
21 D. R. Mott, P. B. Howell, J. P. Golden, C. R. Kaplan, F. S. Ligler and E. S. Oran, *Lab Chip*, 2006, **6**, 540–549.
22 P. B. Howell, D. R. Mott, F. S. Ligler, J. P. Golden, C. R. Kaplan and E. S. Oran, *J. Micromech. Microeng.*, 2008, **18**, 115019(1)–115019(7).
23 D. Mott, P. B. Howell, F. S. Ligler, S. Fertig and A. Bobrowski, *US Pat.*, 20090208372, 2009, p. 25.
24 A. L. Thangawng, P. B. Howell, J. J. Richards, J. S. Erickson and F. S. Ligler, *Lab Chip*, 2009, **9**, 3126–3130.
25 C. Nason, T. Roper, C. Hoyle and J. A. Pojman, *Macromolecules*, 2005, **38**, 5506–5512.